Calcif Tissue Int (2000) 66:355–362

Calcified
Tissue
International
© 2000 Springer-Verlag New York Inc.

Laboratory Investigations

Growth Parameters in the Epiphyseal Cartilage of Brachymorphic (bm/bm) Mice

P. Vanky, U. Brockstedt, M. Nurminen, B. Wikström, A. Hjerpe

Departments of Immunology, Microbiology, Pathology, and Infectious Diseases, Division of Pathology, Karolinska Institute, F42, Huddinge University Hospital, S-141 86, Huddinge, Sweden

Received: 18 December 1998 / Accepted: 30 September 1999

Abstract. We studied kinetics in the epiphyseal cartilage of the brachymorphic (bm/bm) mouse, combining morphometry and labeling with halogenated nucleotides. The defective synthesis of the sulfate donor PAPS in these homozygous mutants is evident in tissues with a large production of glycosaminoglycans; these compounds become undersulfated. Compared with their heterozygous siblings, the longitudinal growth of the mutant mice was reduced by two-thirds. This was mainly associated with (1) reduced height of the proliferating zone, (2) a substantial number of G0 cells in this zone, and (3) reduced hypertrophy which, in turn, may be related to premature mineralization and prevention of normal expansion of cells. No significant effects on cell-cycle parameters were detected, such as S-phase time or cell-cycle time, and the rate at which each cell increased the matrix volume seemed normal. An effect on matrix mineralization may be related to known changes in the structure of matrix PGs, whereas the effect on proliferation may be related to other factors. Candidates for such other effects of undersulfation are the cell surface PGs, which are important for binding of growth factors.

Key words: Epiphyseal cartilage—Growth rate—Brachymorphic mouse—Proliferation—Dwarfism.

Normal longitudinal bone growth depends on several well-regulated events in the epiphyseal cartilage, where the chondrocytes follow a predetermined pattern of differentiation while they "pass through" the growth plate. From a resting pool, where cell metabolism is minimal, they turn into a population of dividing cells, forming the zone of proliferation. The rate of proliferation here is comparable to that in highly malignant tumors. After three to five cell divisions, the chondrocytes leave the cycling stage [1] and, during further maturation, they change their configuration and eventually become hypertrophic, thus forming the zone of hypertrophy. Finally, when the surrounding matrix starts to mineralize, the chondrocytes degenerate and die. The remaining mineralized cartilage matrix then serves as a support for metaphyseal trabecular bone, that subsequently forms, and the production of this matrix then determines the rate of longitudinal bone growth. Several hypotheses have been advanced to explain how mineralization is regulated [2], but the mechanisms by which the proceeding chondrocyte maturation is regulated remain largely unknown.

The chemical structure of the matrix components gives cartilage its special biomechanical properties. The two major constituents of matrix are collagen and proteoglycans (PGs). Three main PGs are present in cartilage matrix. The most abundant in hyaline cartilages is the large PG aggrecan which binds to hyaluronan (HA) and forms huge polyanionic aggregates. The polyanionic nature depends on the chondroitin sulfate (CS) and keratan sulfate (KS) sidechains which are attached to the protein core, forming a "bottle brush" structure. The large number of sulfates and carboxyl groups in these glycosaminoglycans (GAGs) creates an exceptional density of fixed charges in the PG monomer. This charge density then creates a high osmotic pressure which draws water into the tissue and expands the collagen network, thereby giving the tissue shock-absorbing properties essential to the functioning of articular cartilage. Another proposed function of these huge anionic aggregates is to bind considerable quantities of salts such as $CaHPO_4$ and they have thereby been ascribed an important role in the process of mineralization.

Two smaller dermatan sulfate PGs (DSPGs), biglycan and decorin, are also found in cartilage matrix [3]. They both bind to the surface of collagen fibrils, where they are supposed to regulate collagen fibrillogenesis [4, 5]. They also interact with a variety of other macromolecules [6, 7].

Another group of PGs, found on the surface of most cells, including chondrocytes, is the heparan sulfate containing PG family called syndecans. These transmembrane PGs, which bind to a variety of extracellular ligands, including growth factors, play an important role in cell proliferation and differentiation [8].

The volume density (V_V) of cells changes in the growth plate during the differentiation process [9, 10]. The proportion increases slightly from the resting zone to the proliferating and maturation zones, and the increase becomes considerable at the onset of cellular hypertrophy. Although ex-

Correspondence to: A. Hjerpe

tracellular matrix V_V thereby decreases considerably, this mainly represents a reorganization of the tissue, and the amount of matrix varies between the zones. The turnover rates of the main matrix constituents, as measured in other hyaline cartilages, are considerably slower than the rate of epiphyseal plate progression, and the changed composition is therefore the result of new matrix being synthesized.

The brachymorphic (bm/bm) mouse has an autosomal recessive mutation and the phenotype of the homozygous bm/bm mice is characterized by a disproportionate dwarfism [11]. Previous studies on the bm/bm mice have shown an undersulfated cartilage, but normal amounts and types of collagen and glycosaminoglycans [12, 13]. The undersulfation is caused by a mutation in a protein, ATP-sulfurylase-adenosine-5′-phosphosulfate kinase, with two enzymatic activities, a sulfurylase and a kinase site. This mutation impairs the transport or the "channeling mechanism" of the substrate (APS) between the two active sites, thereby reducing the production of PAPS (3′-phosphoadenosine-5′-phosphosulfate) which is the sulfate donor [14–16]. The resulting undersulfation is general, but more pronounced in tissues with a high demand for sulfation, as in cartilage [13, 15, 17]. These mice therefore offer an opportunity to study the importance of PGs in cartilaginous growth and mineralization. The epiphyseal cartilage in these animals has a considerably reduced height and the morphology of this tissue is less ordered in bm/bm mice than in their heterozygous littermates [18]. Thus, the borders between the zones are less distinct, the columnar orientation of chondrocytes is disturbed, and the mineralization is altered. In artificial systems for experimental mineralization, the formation of calcium hydroxyapatite is hampered by aggrecan and this effect is less pronounced with the undersulfated PGs in the bm/bm mice [19].

When studying the turnover of matrix constituents in the epiphyseal growth cartilage, the necessary time intervals for following the incorporation and elimination of these compounds, however, are so long that the rate of progression and altered composition of the growth plate must be considered. In a previous study of normal epiphyseal cartilage we managed to calculate the rate of growth in each zone individually [1]. These data also permit the calculation of the rates by which the matrix volume changes, figures that can be used in studies of matrix metabolism. The rate of growth of the brachymorphic mouse is greatly reduced, although the precise mechanism for this is still poorly understood.

The aim of the present investigation was therefore to elucidate how this decrease in synthesis of PAPS influences the various events in epiphyseal growth, i.e., proliferation, hypertrophy, and mineralization. We also tried to obtain the necessary basis for studies of matrix turnover in the different zones of the growth plate and the importance of PGs in the mineralization process.

Materials and Methods

Animals

All animals were littermates derived from matings between known heterozygous (bm/+) or homozygous (bm/bm) females and homozygous (bm/bm) males (strain B6C3Fe, Jackson Laboratory, Bar Harbor, ME). They were bred with free access to water and standard pelleted food. Only males were included in the study. They were injected intraperitoneally with thymidine analogs at 24–26 days of age, when the growth rate is high. The animals were sacrificed by cervical dislocation at different times after the injections. All experiments were approved by the institutional ethical committee.

Reagents

The specific antibodies employed were anti-BrdUrd (Cat. No. M744, working dilution 1:100) and biotinylated-RAM (Cat. No. E354, working dilution 1:200), both of which were obtained from Dakopatts, (Copenhagen, Denmark), and the IU-4 antibody (Cat. No. MD5010, working dilution 1:10,000) specific for both BrdUrd and IdUrd was obtained from Caltag (South San Francisco, CA). Normal rabbit serum (Cat. No. X0902), streptavidin, and peroxidase-biotin (StreptABC Kit, Cat. No. K377) were all obtained from Dakopatts. The thymidine analogs 5′-iodo-2′-deoxyuridine (IdUrd; Cat. No. I-7125) and 5′-bromo-2′-deoxyuridine (BrdUrd; Cat. No. B-5002) were obtained from Sigma (St. Louis, MO). All other reagents were of analytical grade.

Tissue Preparation

The proximal epiphyseal growth cartilage from the tibia was dissected free from the diaphysis and cut longitudinally into two equal pieces. The tissues were then fixed in phosphate-buffered 4% formalin for 24 hours, decalcified in ethylene-diamine tetraacetic acid (EDTA) for 48 hours, embedded in paraffin, and cut into 4 μm thin sections for further immunohistochemistry. For morphometry, the tissues were instead fixed overnight in 4°C in 2% glutaraldehyde also containing 0.7% safranin-O in 0.1 mol/liter cacodylate buffer (pH 7.4). Postfixation was performed in 2% OsO_4 in 0.15 mol/liter cacodylate and safranin-O (pH 7.4) for 2 hours at 4°C. After dehydration the pieces were embedded through acetone into epoxy resin LX-112 (Ladd Research Industries Inc., Burlington, VT) and 1 μm thin plastic sections were stained with a combination of toluidine blue and von Kossa.

Immunohistochemistry

Endogenous peroxidase activity was extinguished with 0.3% H_2O_2 in methanol for 30 minutes. The sections were then digested for 8 minutes using proteinase K (20 μg/ml in PBS) at room temperature, and the DNA was denaturated with 95% (v/v) formamide in 0.15 mol/liter trisodium citrate for 45 minutes at 68°–70°C, after which the sections were immediately washed in cold Tris-buffered saline (TBS). Nonspecific bindings were blocked with 3% normal rabbit serum for 60 minutes at 4°C.

Incubation with specific antibodies, diluted in 1% normal rabbit serum, was performed overnight at 4°C. Negative controls were obtained by excluding the specific antibody. Reactivity to specific antibodies was monitored with the StreptABC technique, using a biotinylated rabbit-antimouse antibody, and diaminobenzidine (DAB). The sections were counterstained with hematoxylin.

Experiments

To detect S-phase cells and follow their redistribution with time, 47 bm/bm and 47 control (bm/+) mice were given an intraperitoneal injection with IdUrd (50 mg/kg body weight), dissolved in physiologic saline. They were sacrificed at various intervals after injection, using five animals for each of the 1.5, 10, 24, 36, 48, 72, and 96 hour intervals, and two animals for each of the 1, 2, 4, 6, 8, and 12 hour intervals. The proximal tibial epiphysis from each animal was divided into halves and embedded in paraffin, taking one block per animal for further analysis. The proportion of labeled nuclear profiles was estimated on the basis of light microscopy (LM) micrographs (260× and 520× for calculation of labeled and unlabeled cells, respectively), with a minimum of 400 counted cell profiles per animal. In these sections, the cytoplasm was readily identified, whereas a negative nucleus faintly stained with hematoxylin could be difficult to distinguish. To facilitate determination of the total number of nuclear profiles, we estimated, as

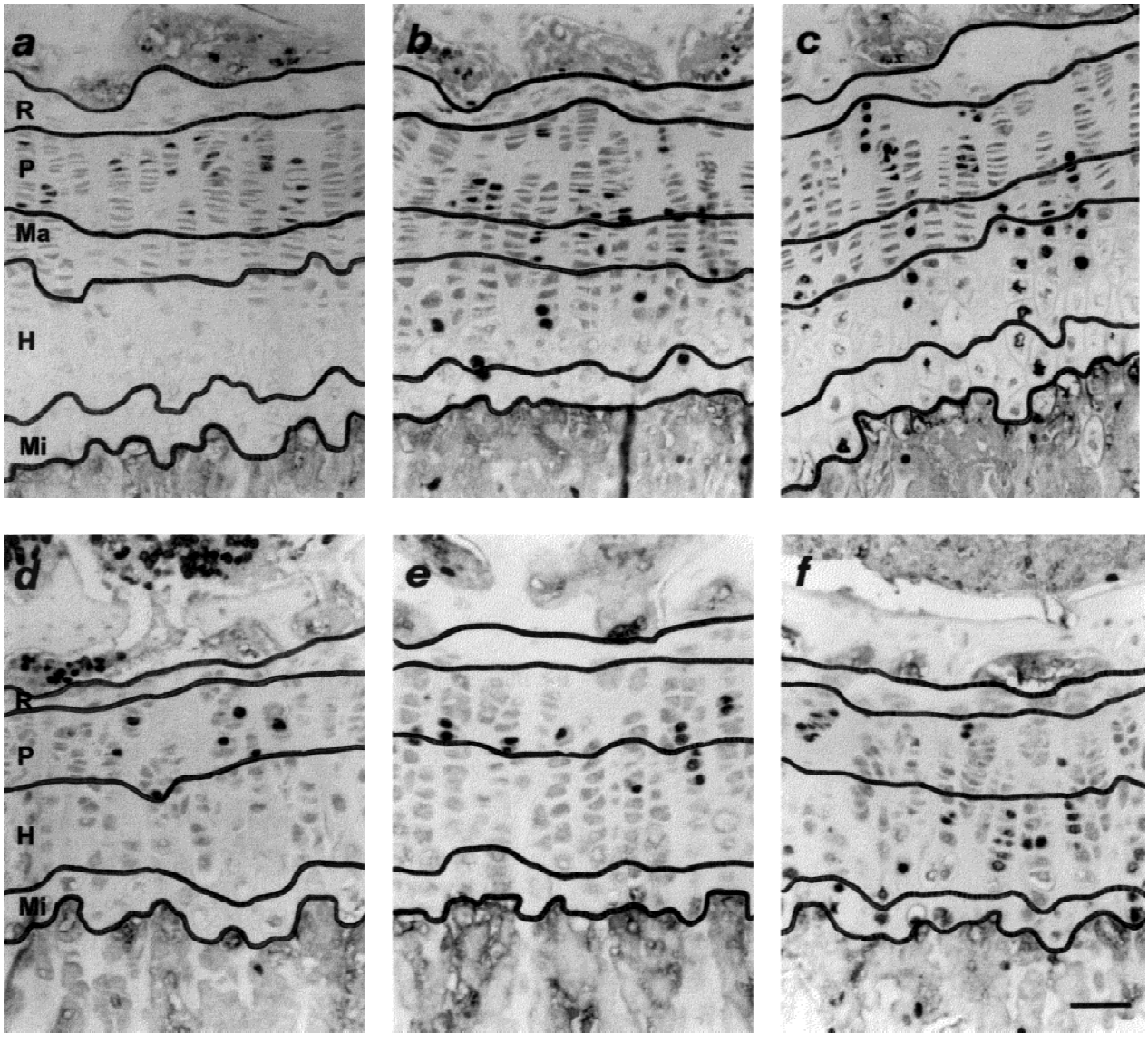

Fig. 1. LM micrographs (magnification ×180) show the distribution of immunoreactive chondrocytes in bm/+ mice (**a–c**) and in bm/bm mice (**d–f**) after injection of IdUrd at 1.5 hours (**a** and **d**), 24 hours (**b** and **e**), and 72 hours (**c** and **f**), respectively. No zone of maturation could be defined in the bm/bm mice. Most of the labeled chondrocytes are lying two and two after 24 hours showing that they have passed one mitosis. After 24 hours in bm/+ mice and after 36 hours in bm/bm mice (not shown) positively stained nuclei were seen at the chondro-osseus junction. R = resting zone; P = proliferating zone; Ma = maturation zone; H = hypertrophic zone; Mi = mineralizing zone. Bar represents 50 μm.

in our previous study, a correction factor for each zone to permit the calculation of nuclear profiles based on the number of cytoplasmic profiles detected [1]. In the control tissue, these correction factors were 0.77, 0.67, 0.75, and 0.78 for the proliferating, maturation, hypertrophic, and mineralizing zones, respectively. In the mutant mice, where no maturation zone could be distinguished, the corresponding factors for proliferating, hypertrophic, and mineralizing zones were 0.81, 0.80, and 0.80, respectively.

To estimate the proportion of G0 cells in the proliferating zone, four bm/bm and four control animals were injected repeatedly with IdUrd, each time using 50 mg/kg b.w. Eight injections were given to each animal at 6-hour intervals over a period of 42 hours sacrificing them 1.5 hours after the last injection. The length of the intervals (6 hours) was chosen to be shorter than the S-phase and the whole labeling period (42 hours) was chosen to be longer than the assumed G2 + M + G1-phase together to ensure labeling of all proliferating cells.

To determine the duration of the S-phase, seven bm/bm mice and five controls were first injected with IdUrd 50 mg/kg b.w. and 1 hour later with BrdUrd 50 mg/kg b.w., and they were sacrificed after 1 more hour. Two parallel sections from each paraffin block were taken for immunohistochemistry. One section was incubated with an antibody (Anti-BrdUrd) specific for BrdUrd alone and the parallel section with another antibody (Iu-4) which reacts with equally high affinity for both BrdUrd and IdUrd. The labeling index (LI) for the corresponding areas in the proliferating zone was then calculated using micrographs taken from the two parallel sections. Differences in LI between the two sections represent the proportion of chondrocytes leaving the S-phase during the interval between the two injections, in this case, 1 hour.

Morphometric analysis was performed on 1 μm thin plastic sections from five bm/bm and five controls. LM micrographs (final magnification of 1025×) were taken, using one section from each animal. In the control animals, the borders between zones were

delineated with the same definitions as previously used [1, 20, 21]. A maturation zone could not be defined in the mutant mice. Instead, cellular hypertrophy appeared close to the last proliferating cells, with an indistinct border between the zones. In both controls and mutants the proliferating and hypertrophic zones were further divided into two halves. To determine the height of each zone and subzone, as defined above, vertical measurements were performed after systematized randomization on the LM prints. More than 200 measurements were made in each zone (minimum of 40 measurements per animal and zone). The longitudinal distances between cell centers were determined at the different zone borders by measuring the distance between three cells in the same column (in the mineralizing zone, two cells), using the upper cell membrane as the point of measurement. The average number of cells per column and zone/subzone was calculated by dividing the height of the zone by the average distance between cell centers in the same zone.

The volume densities of cells and matrix were measured at the various zone borders, where an area was defined on the micrographs, ranging from 1 cm above to 1 cm below this border (final magnification of 1025×). Calculations were performed by the point-counting method of Weibel [22], using square lattices of 1 cm and 2 cm superimposed on the micrographs.

Statistics

Obtained differences were evaluated using Student's *t*-test at a rejection level of 5%.

Results

Zone Heights, Cell Numbers, and Cell-Center Distances

The entire calculation of tissue turnover is based on the structure, where the number of cells per column and changes in distances between cells are crucial. The height of the total growth plate in the bm/bm mice is greatly reduced and measures only 62% of that in the control animals. Although most evident in the lower part of the plate (Fig. 2), all zones are affected (Table 1 and Fig. 1) and the borders between zones were so uneven that a zone of maturation could not be delineated in the mutant mice. The calculation of the number of cells per column shows that, while the normal animals have an average of 33.5, the bm/bm have only 20.4 cells/column. The reduction in cell number is greatest in the proliferating zone (Table 1). The distances between cell centers in the mineralizing zone were also reduced from 22.1 ± 0.5 μm (SEM) to 17.2 ± 0.5 μm (SEM) Fig. 3). These results are in good accordance with earlier reports [11, 18].

Presence of G0 Cells in the Proliferating Zone

For the estimation of cell-cycle parameters it is necessary to consider the true number of cycling cells. As in our previous study of normal mice [1], almost all chondrocytes in the proliferating zone of the bm/+ animals were once in S-phase during the time interval (42 hours) when repeated IdUrd injections were given. In these animals, only 5.0 ± 0.2% (SEM) were negative, indicating a low proportion of G0 cells. In the bm/bm mice, a significantly higher proportion—22.1 ± 2.1% (SEM)—of the chondrocytes in the proliferating zone remained negative. This means that more than one-fifth of the cells do not cycle, i.e., are in G0 or less probably have a G1 + M + G2-time longer than 42 hours. Assuming they are in G0, two to three of all the 10.5 proliferating cells per average column (Table 1) do not take part in proliferation.

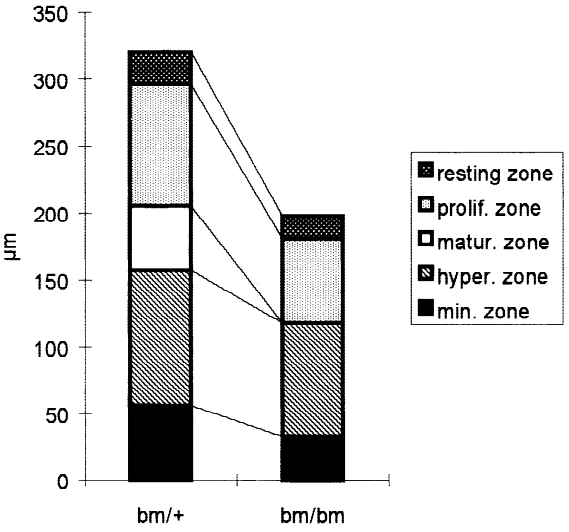

Fig. 2. A comparison between zone heights, showing that the whole epiphyseal plate, i.e., all of the zones, are affected in the bm/bm mice. The total height of the plate is reduced by more than one-third.

S-Phase Times and Cell-Cycle Times

The growth rates are calculated by relating the structural parameters to the times for s-phase and total cell-cycle. The percentages of labeled nuclear profiles (labeling index, LI) in the proliferating zone differed somewhat between controls and bm/bm—17.8 ± 0.2% (SEM) and 13.7 ± 1.1% (SEM), respectively. The LI in the proliferating zone also represents the proportional duration of the S-phase in an average cell cycle, if a correction for nonproliferating cells has been made. The double-labeled (first IdUrd and 1 hour later BrdUrd) animals were used to calculate the duration of S-phases. In control mice, 15.6 ± 0.5% (SEM) of the labeled nuclear profiles left the S-phase during 1 hour, while the corresponding figure for bm/bm was 14.5 ± 1.5% (SEM). This gives average S-phase times of 1.0 hour/0.156 = 6.4 hours and 1.0 hour/0.145 ± 6.9 hours for bm/+ and bm/bm, respectively. By relating these times to LIs and to the proportion of proliferating cells (0.95 and 0.78, respectively), we found an average cell-cycle time of 0.95 × 6.4 hours/0.178 = 34.2 hours in the controls and 0.78 × 6.9/0.137 = 39.3 hours in the bm/bm mice. Thus, the percentages of cells in the proliferating zone that undergo mitosis are 100 × 0.178/6.4 = 2.8% per hour and 100 × 0.137/6.9 = 2.0% per hour for controls and mutant mice, respectively. Most of this difference, however, is associated with differences in the percentages of proliferating cells, the corresponding mitotic rates among proliferating chondrocytes being 2.8%/0.95 = 2.9% per hour and 2.0%/0.78 = 2.5% per hour, respectively. Therefore, there are no significant differences in S-phase time or in the average cell-cycle time between normal and dwarf mice.

Graphic Determination of S-Phase Times and G2 + M-Phase Times

Plotting the LIs at shorter and more frequent time intervals permits a graphic estimation of the S-phase times and G2 + M-phase times (Fig. 4). After injection, a shorter interval

Table 1. Vertical cell-center distances at the upper border of each zone

	bm/+				bm/bm			
	Height of zone (μm ± SEM)	Cell-center distance (μm ± SEM)	Δ Cell-center distance (μm)	Number of cells per average column	Height of zone (μm ± SEM)	Cell-center distance (μm ± SEM)	Δ Cell-center distance (μm)	Number of cells per average column
Proliferating zone	91.3 ± 1.4	3.86 ± 0.15	2.49	18.0[a]	63.0 ± 0.8[b]	5.14 ± 0.23[b]	2.19	10.5[a]
Maturation zone	47.7 ± 1.0	6.34 ± 0.25	3.40	5.9	—	—	—	—
Hypertrophic zone	101 ± 1.4	9.74 ± 0.28	10.6	6.9[a]	85.3 ± 1.1[b]	7.33 ± 0.36[b]	9.23	8.0[a]
Mineralizing zone	55.7 ± 1.0	20.3 ± 0.6	1.8	2.6	32.5 ± 0.8[b]	16.6 ± 0.6[b]	0.7	1.9
Total	296 ± 2	22.1 ± 0.5	18.2	33.5	181 ± 2[b]	17.2 ± 0.5[b]	12.1	20.4

[a] Calculations based on measurements in subdivided zones
[b] Statistically different from the corresponding bm/+ value

Table 2. Growth rates

	bm/+			bm/bm		
	Cell proliferation (μm/h)	Cell hypertrophy (μm/h)	Total growth (μm/h)	Cell proliferation (μm/h)	Cell hypertrophy (μm/h)	Total growth (μm/h)
Proliferating zone	1.93	1.24	3.17	1.08	0.46	1.54
Maturation zone	0	1.70	1.70	—	—	—
Hypertrophic zone	0	5.29	5.29	0	1.94	1.94
Mineralizing zone	0	0.90	0.90	0	0.14	0.14
Total growth	1.93	9.13	11.06	1.08	2.54	3.62

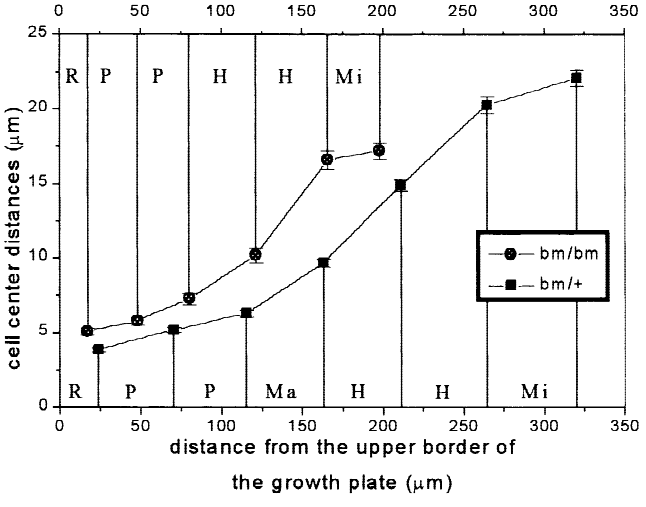

Fig. 3. Cell-center distances at the lower border of each zone and at the center of the proliferating and hypertrophic zones in both bm/+ and bm/bm mice. The final cell-center distance in the mutant mice corresponds to the cell-center distance in the middle of the hypertrophic zone in the normal mice. R = resting zone; P = proliferating zone; Ma = maturation zone; H = hypertrophic zone; Mi = mineralizing zone. Bars denote SEM.

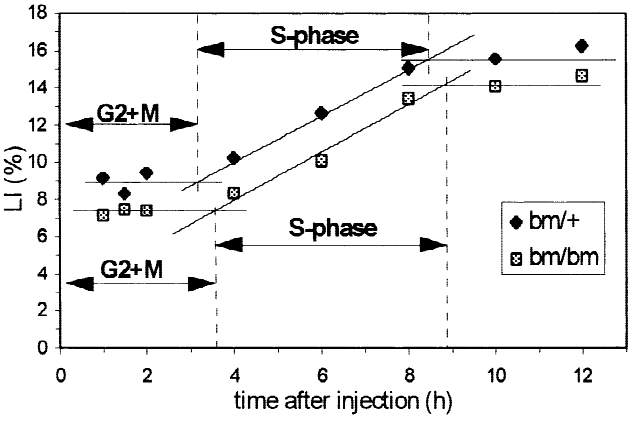

Fig. 4. The total LIs (including the whole growth plate) obtained at shorter intervals after injection in bm/+ and bm/bm mice. An extrapolation of the curves gives no significant differences in G2 + M-phase and S-phase duration between the mutant and the normal mice, the G2 + M-phase duration being 3–3.5 hours and the S-phase 5.5–6 hours.

with constant LI is expected, corresponding to the G2 + M-phase time. This time is followed by a linear increase in LI, equal to the S-phase time, ended by a plateau representing the G1-phase. The S-phase time, estimated graphically, were around 5.5–6 hours in both bm/+ and bm/bm mice and are in accordance with the above calculated figures. The G2 + M-phase times were about 3–3.5 hours and did not differ significantly between controls and mutants.

Progression of Labeled Cells

Immunoreactive cells could be followed on their way through the growth plates at different times after injection (1.5–96 hours) (Fig. 5). A doubling of the LIs occurred after

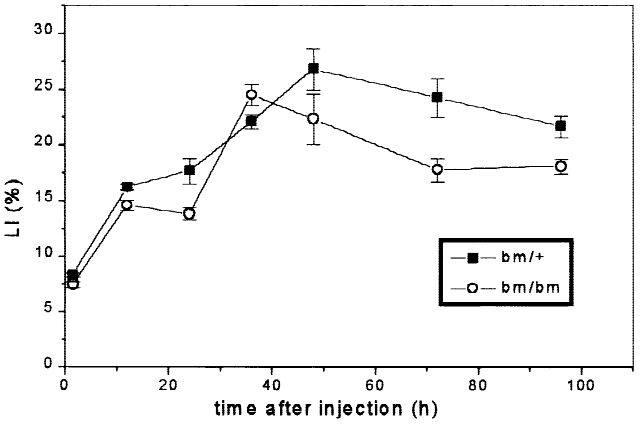

Fig. 5. The total LIs (including the whole growth plate) obtained at longer intervals (1.5–96 hours). In both bm/+ and bm/bm mice, the LIs are doubled after 12 hours, i.e., all labeled cells have passed one mitosis. Both curves reach a first plateau after 12 hours, indicating that the labeled cells are not dividing. The gradual increase in control mice between 24 and 48 hours is probably due to variations in the cell-cycle time. A maximum in LIs is seen after 36 and 48 hours in bm/bm and bm/+ mice, respectively. The following decline is associated with a decreased amount of labeled cells in the proliferating zone and resorption of labeled cells at the chondro-osseous junction. Bars denote SEM.

10–12 hours in bm/+ and bm/bm animals, which means that every labeled cell has passed a mitosis during this interval, corresponding to the S + G2 + M-phases. This seems reasonable compared with the aforementioned estimate of S-phase times, i.e., approximately 6.5–7 hours. The LI plateau, obtained in both groups of animals between 12 and 24 hours, indicates that all labeled cells are in G1, S, or G2. The subsequent increase, seen after 24 hours, indicates that chondrocytes with the shortest cell-cycles pass their second mitosis already after 24 hours, demonstrating a variation in cycle time.

The proportion of labeled nuclear profiles starts to decline after 48 and 36 hours in bm/+ or bm/bm, respectively. This is associated with reduced amounts of labeled cells in the proliferating zone, while labeled cells are resorbed at the condro-osseous junction. The first immunoreactive cells were detected in the mineralizing zone as soon as 24 hours after IdUrd injection in control animals (Fig. 1b) and after 36 hours in the bm/bm.

Estimates of Longitudinal Growth Rates

The rate of enchondral bone growth can be described as the result of two processes in the epiphyseal plate—proliferation and hypertrophy of the chondrocytes. Cell division takes place only in the proliferating zone where the columnar height is 18.0 chondrocytes in normal mice and 10.5 chondrocytes in mutant mice. Thus, the longitudinal expansion of the plate due to proliferation in bm/+ mice corresponds to a height of $18.0 \times 0.028 = 0.50$ cells per hour and column, and in bm/bm mice to $10.5 \times 0.020 = 0.21$ cells per hour and column.

From the values for cell proliferation and cell-center distances, one can estimate the growth rate, expressed as microns per hour, and this can be performed at any chosen level in the growth cartilage (Table 2). The total growth can be estimated from the rate of cell proliferation and the final cell-center distance at the cartilage-bone junction. In the upper tibial epiphysis of 25-day-old normal mice, this total growth is 11.1 μm/hour, whereas it is only one-third of that (3.6 μm/hour) in the mutant animals. All differences between the two groups are statistically significant. In both bm/+ and bm/bm mice, the process of hypertrophy constitutes the major factor, 83% and 70%, respectively. This is in good accordance with previous findings in normal animals [1, 23, 24].

Estimates of Changes in Matrix Volume

By combining data regarding longitudinal expansion in the various zones and data concerning volume density of extracellular matrix, one can calculate the change in volume of matrix per unit area of the growth plate. When the volumes are calculated as the compartment surrounding each cell, it is seen that the matrix volume increases continuously from the proliferating zone through the hypertrophic zone in both the mutant and control mice (Table 3). This is in accordance with previous studies on matrix synthesis and a higher amount of organelles coupled to matrix synthesis in hypertrophic cells than in proliferating cells [9, 10]. In the mineralizing zone, a decrease is seen, particularly in the controls, probably due to a reduced matrix synthesis parallel with a continuation of high matrix breakdown [25]. These figures also revealed that each hypertrophic cell in bm/bm mice has almost twice as much surrounding matrix as the corresponding cell in bm/+ mice.

One can also estimate the rate of this change per unit area by comparing the findings at the upper and lower borders of each zone. The differences in matrix volume per cell compartment at these borders are obtained from the distances between cell centers and the corresponding volume densities of the matrix. The estimates obtained are then multiplied by the cell-center distances to obtain the matrix volume per cell compartment (V_{cell}). The proliferation rate in bm/+ and bm/bm of 0.50 and 0.21 new cells per column and hour, respectively, then gives the average rate of volume expansion per zone (ΔV_{zone}) as $(V_{lower\ cell} - V_{upper\ cell}) \times 0.50$ or 0.21, where $V_{lower\ cell}$ and $V_{upper\ cell}$ represent the matrix volume compartments related to the first and last cell in the zone. The expansion rate in the proliferating zone is obtained when $V_{upper\ cell} = 0$. The average increase per cell and hour in each zone (ΔV_{cell}) is then calculated by dividing by the number of cells ($\Delta V_{zone}/n$) (Table 3).

No difference was seen between the two mouse types in the chondrocytes' ability to increase their matrix production (ΔV_{cell}).

Discussion

We have used a model for estimating the longitudinal bone growth, described in an earlier paper [1], where a combination of the determined proliferation rate and the measured cell-center distances, at any level of interest in the growth cartilage, permits calculation of the actual growth rate. Our results show that longitudinal bone growth in brachymorphic mice is less than one-third of that in control mice. The reduced longitudinal growth in the bm/bm mice is mainly the result of (1) a narrower proliferating zone, leading to fewer proliferating cells per column, (2) more than one-fifth of the cells in the proliferating zone seem to be in G0 and

Table 3. Rates of change in matrix volume in bm/+ and bm/bm mice

bm/+

	Number of cells per column (n)	Cell-center distances at lower border (μm ± SEM)	Vv of matrix at lower border (±SEM)	Matrix volume per cell compartment[a]	Increase in volume per cell compartment[a] (V_{cell})	Increase in volume per zone and hour[b] (ΔV_{zone})	Increase in volume per cell and hour[b] (ΔV_{cell})
Proliferating zone	18.0	6.34 ± 0.25	0.615 ± 0.013	3.90	3.90	1.95	0.11
Maturation zone	5.9	9.74 ± 0.28	0.509 ± 0.028	4.96	1.06	0.53	0.09
Hypertrophic zone	6.9	20.3 ± 0.6	0.286 ± 0.017	5.81	0.85	0.42	0.06
Mineralizing zone	2.6	22.1 ± 0.5	0.200 ± 0.013	4.43	−1.38	−0.69	−0.26

[a] Nanoliters per sq. millimeters of epiphyseal cartilage area
[b] Nanoliters per sq. millimeters of epiphyseal cartilage area and hour

Bm/bm

	Number of cells per column (n)	Cell-center distances at lower border (μm ± SEM)	Vv of matrix at lower border (±SEM)	Matrix volume per cell compartment[a]	Increase in volume per cell compartment[a] (V_{cell})	Increase in volume per zone and hour[b] (ΔV_{zone})	Increase in volume per cell and hour[b] (ΔV_{cell})
Proliferating zone	10.5	7.33 ± 0.36	0.608 ± 0.006[c]	4.45	4.45	0.94	0.09
Hypertrophic zone	8.0	16.6 ± 0.6[c]	0.486 ± 0.024[c]	8.04	3.59	0.75	0.09
Mineralizing zone	1.9	17.2 ± 0.5[c]	0.462 ± 0.015[c]	7.95	−0.10	−0.02	−0.01

[a] Nanoliters per sq. millimeters of epiphyseal cartilage area
[b] Nanoliters per sq. millimeters of epiphyseal cartilage area and hour
[c] Statistically different from the corresponding bm/+ value

consequently do not proliferate and, (3) the final cellular hypertrophy, constituting the major factor in longitudinal growth, is reduced by more than 20%. The difference is due not to changes in cell-cycle parameters or proliferation rate, since estimates showed only insignificant changes in cell-cycle times and the increases in matrix volume per cell and hour were similar in both groups.

The reduced hypertrophy in bm/bm mice, measured as shorter final cell-center distance, is either the result of a decreased capacity for hypertrophy or the result of premature mineralization preventing an adequate hypertrophy. The latter of these two is supported by earlier findings that undersulfated PGs in cartilage are less effective inhibitors of hydroxyapatite formation than normally sulfated PGs [19], which may result in an earlier mineralization front in bm/bm mice. The height of the growth plate in 25-day-old bm/bm mice is around 200 μm and the final cell-center distance is 17 μm. If we measure this distance between cells in the control mice at the same level, 200 μm from the epiphysis—i.e., in the middle of the hypertrophic zone—the cell-center distance there, 15 μm, is close to the final measurement in the mutant mice; in fact, this distance is even slightly larger in the bm/bm mice (Fig. 3). This would support the hypothesis that the reduced hypertrophy in bm/bm mice may be a result of too early mineralization.

The decreased capacity to sulfate GAGs should affect not only the aggrecan but also other PGs, such as the membrane-bound PGs of the syndecan family. The syndecans play an important role in cell proliferation and differentiation, as one of their known functions is to bind different growth factors and act as cell-surface co-receptors [8, 26–28]. These bindings depend on HS sequences with a specific sulfation pattern [29], and an overall disturbance of the sulfation should therefore also affect the ability of syndecans to present growth factors to their high-affinity receptors. This may explain a narrower proliferating zone and an increased amount of chondrocytes in G0 in the proliferating zone, a hypothesis also supported by studies showing that cartilage of bm/bm mice contains lower amounts of bFGF than cartilage or normal bm/+ [30] and that a selective desulfation of heparin chains results in an impaired mitogenic activity of the fibroblast growth factor (FGF) *in vitro* [31].

In previous studies of cell kinetics in growth cartilage of different dwarf mutations in mice [32–34], the heterozygous normal phenotypes showed great similarity to the present study concerning the height of the epiphyseal cartilage, number of cells per column, maximum height of hypertrophied cells, and LI in the proliferating zone. The calculated growth rate (11.1 μm/hour) in the present study, however, was about twice as high as those calculated previously because of the differences in S-phase times, resulting in different average cell-cycle times. In this study, the S-phase time (6.4 hours) was measured as described above, whereas in previous studies, the growth rates seem to be based on an assumed, excessively long, S-phase time.

The ability of chondrocytes to synthesize matrix in the bm/bm mice seems to be no worse than in bm/+ mice, in fact, they synthesize about the same matrix volume per cell and hour. Both the bm/+ and bm/bm mice show a gradual increase in matrix volume per cell compartment from the proliferating to the hypertrophic zone. The increase in the bm/+ mouse, which is a normal phenotype, is lower in the present study than in our earlier study, made on normal NMRI mice [1]. The difference in matrix volume per cell compartment relates to differences in matrix V_v. In our earlier study, the matrix V_vs used were obtained by extrapolation of zonal mean values; in the present study, these V_vs were measured also at the zone borders, these figures being more accurate and relevant to the subsequent calculations.

A large number of human chondrodystrofies have been identified based on clinical, genetical, radiological, and histological findings. None of these have so far been linked to

defect sulfation as in the bm/bm mice. The histological findings in the epiphyseal growth plates of the most common of these human conditions—achondroplasia—show considerable morphological similarity to the findings in bm/bm. Achondroplasia has been associated with mutations in the FGF receptor-3 (FGFR-3) [35], demonstrating the importance of FGF interactions for the proliferation of epiphyseal chondrocytes. The precise effect of these interactions is, however, by no means clear, and it has even been suggested that the FGFR-3 receptor is a negative regulator of skeletal growth [35]. The disturbed hypertrophy and mineralization in the human conditions may indicate that this growth factor is also important to the production and turnover of matrix PGs. These events are, however, complex and further studies, using transgenic and other models, are necessary to explain this regulation. The present way to characterize epiphyseal kinetics may offer crucial information in such studies.

References

1. Vanky P, Brockstedt U, Hjerpe A, Wikström B (1998) Kinetic studies on epiphyseal growth cartilage in the normal mouse. Bone 22:331–339
2. Howell DS, Dean DD (1992) The biology, chemistry, and biochemistry of the mammalian growth plate. In: Coe FL, Favus MJ (eds) Disorders of bone and mineral metabolism. Raven Press Ltd, New York, p 313
3. Bianco P, Fisher LW, Young MF, Termine JD, Robey PG (1990) Expression and localization of two small proteoglycans, biglycan and decorin, in developing human skeletal and non-skeletal tissues. J Histochem Cytochem 38:1549–1563
4. Scott JE (1988) Proteoglycan-fibrillar collagen interactions. Biochem J 252:313–323
5. Vogel KG, Paulsson M, Heinegård D (1984) Specific inhibition of type I and type II collagen fibrillogenesis by the small proteoglycan of tendon. Biochem J 223:587–597
6. Yamaguchi Y, Mann DM, Ruoslahti E (1990) Negative regulation of transforming growth factor-β by the proteoglycan decorin. Nature 346:281–284
7. Lewandowska K, Choi HU, Rosenberg LC, Zardi L, Culp LA (1987) Fibronectin-mediated adhesion of fibroblasts: inhibition by dermatan sulfate proteoglycan and evidence for a cryptic glycosaminoglycan-binding domain. J Cell Biol 105:443–454
8. Carey DJ (1997) Syndecans: multifunctional cell-surface coreceptors. Biochem J 327:1–16
9. Buckwalter JA, Mower D, Ungar R, Schaeffer J, Ginsberg B (1986) Morphometric analysis of chondrocyte hypertrophy. J Bone Jt Surg 68-A:243–255
10. Hunziker EB, Schenk RK, Cruz-Orive L-M (1987) Quantitation of chondrocyte performance in growth-plate cartilage during longitudinal bone growth. J Bone Jt Surg 69-A:162–173
11. Lane PW, Dickie MM (1968) Three recessive mutations producing disproportionate dwarfing in mice. J Hered 59:300–308
12. Orkin RW, Pratt RM, Martin GR (1976) Undersulfated chondroitin sulfate in the matrix of brachymorphic mice. Dev Biol 50:82–94
13. Pennypacker JP, Kimata K, Brown KS (1981) Brachymorphic mice (bm/bm): a generalized biochemical defect expressed primarily in cartilage. Dev Biol 81:280–287
14. Lyle S, Stanczak JD, Westley J, Schwartz NB (1995) Sulfate-activating enzymes in normal and brachymorphic mice: evidence for a channeling defect. Biochemistry 34:940–945
15. Schwartz NB (1982) Defect in proteoglycan synthesis in brachymorphic mice. Prog Clin Biol Res 110:97–103
16. Schwartz NB, Lyle S, Ozeran JD, Li H, Deyrup A, Ng K, Westley J (1998) Sulfate activation and transport in mammals: system component and mechanisms. Chem Biol Interact 109: 143–151
17. Yamada K, Shimizu S, Brown KS, Kimata K (1984) The histochemistry of complex carbohydates in certain organs of homozygous brachymorphic (bm/bm) mice. Histochem J 16: 587–599
18. Orkin RW, Williams BR, Cranley RE, Poppke DC, Brown KS (1977) Defects in the cartilaginous growth plate of brachymorphic mice. J Cell Biol 73:287–299
19. Boskey AL, Maresca M, Wikström B, Hjerpe A (1991) Hydroxyapatite formation in the presence of proteoglycans of reduced sulfate content: studies in the brachymorphic mouse. Calcif Tissue Int 49:389–393
20. Reinholt FP, Engfeldt B, Hjerpe A, Jansson K (1982) Stereological studies on the epiphyseal growth plate with special reference to the distribution of matrix vesicles. J Ultrastruct Res 80:270–279
21. Wikström B, Hjerpe A, Jansson K, Reinholt FP, Engfeldt B (1984) Stereological analysis of the epiphyseal growth cartilage in the brachymorphic (bm/bm) mouse with special reference to the distribution of matrix vesicles. Virch Arch 47:199–210
22. Weibel ER (1979) Stereological methods, vol. 1. Practical methods for biological morphometry. Academic Press, London, New York
23. Breur GJ, Van Enkevort BA, Farnum CE, Wilsman NJ (1991) Linear relationship between the volume of hypertrophic chondrocytes and the rate of longitudinal bone growth in growth plates. J Orthop Res 9:348–359
24. Wilsman NJ, Farnum CE, Green EM, Lieferman EM, Clayton MK (1996) Cell cycle analysis of proliferative zone chondrocytes in growth plates elongating at different rates. J Bone Jt Surg 14:562–572
25. Shapses SA, Sandell LJ, Ratcliffe A (1994) Differential rates of aggrecan synthesis and breakdown in different zones of the bovine growth plate. Matrix Biol 14:77–86
26. Chintala SK, Miller RR, McDevitt CA (1995) Role of heparan sulfate in the terminal differentiation of growth plate chondrocytes. Arch Biochem Biophys 316:227–234
27. Salmivirta M, Heino J, Jalkanen M (1992) Basic fibroblast growth factor-syndecan complex at cell surface or immobilized to matrix promotes cell growth. J Biol Chem 267:17606–17610
28. Shimazu A, Nah H-D, Kirsch T, Koyama E, Leatherman JL, Golden EB, Kosher RA, Pacifici M (1996) Syndecan-3 and the control of chondrocyte proliferation during endochondral ossification. Exp Cell Res 229:126–136
29. Turnbull JE, Fernig DG, Ke Y, Wilkinson MC, Gallagher JT (1992) Identification of the basic fibroblast growth factor binding sequence in fibroblast heparan sulfate. J Biol Chem 267:10337–10341
30. Wezeman FH, Bollnow MR (1997) Immunohistochemical localization of fibroblast growth factor-2 in normal and brachymorphic mouse tibial growth plate and articular cartilage. Histochem J 29:505–514
31. Ishihara M, Takano R, Kanda T, Hayashi K, Hara S, Kikuchi H, Yoshida K (1995) Importance of 6-O-sulfate groups of glucosamine residues in heparin for activation of FGF-1 and FGF-2. J Biochem 118:1255–1260
32. Sannasgala SSMMK, Johnson DR (1990) Kinetic parameters in the growth plate of normal and achondroplastic (cn/cn) mice. J Anat 172:245–258
33. Thurston MN, Johnson DR, Kember NF (1985) Cell kinetics of growth cartilage of achondroplastic (cn) mice. J Anat 140: 425–434
34. Thurston MN, Johnson DR, Kember NF, Moore WJ (1983) Cell kinetics of growth cartilage in stumpy: a new chondrodystrophic mutant in the mouse. J Anat 136:407–415
35. Bonaventure J, Rosseau F, Legeai-Mallet L, Le Merrer M, Munnich A, Maroteaux P (1996) Common mutations in the gene encoding fibroblast growth factor receptor 3 account for achondroplasia, hypochondroplasia and thanatophoric dysplasia. Acta Pædiatr (suppl)417:33–38